ChemPhysChem

Research Article
doi.org/10.1002/cphc.202200729

Chemistry Europe
European Chemical Societies Publishing

www.chemphyschem.org

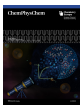

Activity-Based Models to Predict Kinetics of Levulinic Acid Esterification

Marcel Klinksiek,[a] Sindi Baco,[b, c] Sébastien Leveneur,[b] Julien Legros,[c] and Christoph Held*[a]

The solvent is of prime importance in biomass conversion as it influences dissolution, reaction kinetics, catalyst activity and thermodynamic equilibrium of the reaction system. So far, activity-based models were developed to predict kinetics and equilibria, but the influence of the catalyst on kinetics has not been succesfully predicted by thermodynamic models. In this work, the thermodynamic model ePC-SAFT advanced was used to predict the activities of the reactants and of the catalyst at various conditions (temperature, reactant concentrations, γ-valerolactone GVL cosolvent addition, catalyst concentration) for the homogeneously acid-catalyzed esterification of levulinic acid (LA) with ethanol. Different kinetic models were applied, and it was found that the catalyst influence on kinetics could be predicted correctly by simultaneously solving the dissociation equilibrium of H_2SO_4 catalyst along the reaction coordinate and by relating reaction kinetics to proton activity. ePC-SAFT advanced model parameters were only fitted to reaction-independent phase equilibrium data. The key reaction properties were determined by applying ePC-SAFT advanced to one experimental kinetic curve for a set of temperatures, yielding the reaction enthalpy at standard state $\Delta^R H^0 = 11.48\ kJ\ mol^{-1}$, activation energy $E_A = 30.28\ kJ\ mol^{-1}$ and the intrinsic reaction rate constant $k = 0.011\ s^{-1}$ at 323 K, which is independent of catalyst concentration. The new procedure allowed an a-priori identification of the effects of catalyst, solvent and reactant concentration on LA esterification.

Introduction

The chemical industry is dealing with emerging environmental issues and depletion of fossil resources. In recent years, intensive research fields have emerged to identify attractive renewable energy and material resources.[1] Within this context, the utilization of lignocellulosic biomass has become a potential alternative for sustainable production of chemicals and fuels.[2–5] One chemical of special attention is levulinic acid (LA), as this compound and its derived esters have a formidable potential as a renewable feedstock for the synthesis of several chemicals for applications in fuel additives, fragrances, solvents and pharmaceuticals.[5,6] One ester of interest as fuel additive and a potential biomass-derived platform molecule is ethyl levulinate (ELA).[7] ELA is synthesized by an esterification reaction of LA with an excess amount of ethanol. Research on esterification of levulinic acid has been investigating catalyst screening[8] and effect of reactant molar ratio[9] and catalyst concentration[10] on the reaction rate. However, there is a lack of predicting the LA esterification kinetics in the literature. In this work, the esterification is considered in the liquid phase at the presence of the acid catalyst H_2SO_4 according to Eq. (1).

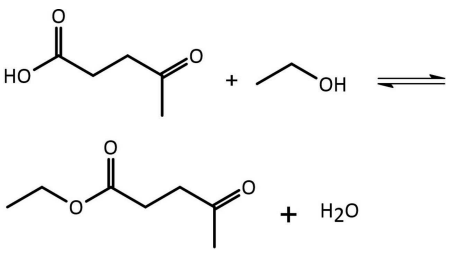

(1)

Motivated by the recent research focus on ELA, this work aims at a more detailed discussion on the role of solvent and catalytic properties on the ELA reaction. For this purpose, the kinetics of LA esterification with ethanol with an additional renewable and non-toxic solvent was studied in this work. In the literature, one organic solvent which was found to have an impact on reaction rates is γ-valerolactone (GVL).[11] GVL has a low toxicity and can be obtained without consumptions of fossil resources,[12] thus it is considered to be a green solvent. Further, within the esterification reaction the protonation of the carboxyl group is the rate-determining step and needs activation either by temperature or by a catalyst.[10] The kinetics of an acid-catalyzed esterification of LA to ELA in a temperature range of 50 to 80 °C was investigated in batch reactor by Baco et al.[13] Although that study explored several conditions on kinetics, still it lacks in knowledge on the catalyst properties

[a] M. Klinksiek, Dr. C. Held
Laboratory of Thermodynamics, Department of Biochemical and Chemical Engineering, TU Dortmund University
Emil-Figge-Str. 70, 44227 Dortmund, Germany
E-mail: christoph.held@tu-dortmund.de
[b] S. Baco, Prof. S. Leveneur
INSA Rouen, UNIROUEN,
Normandie Univ, LSPC
UR4704, 76000 Rouen, France
[c] S. Baco, Prof. J. Legros
INSA Rouen, CNRS
Normandie Université, UNIROUEN
COBRA laboratory, 76000 Rouen, France

Supporting information for this article is available on the WWW under https://doi.org/10.1002/cphc.202200729

during the reaction coordinate, such as catalyst dissociation and molecular interactions of the catalyst. Activity-based approaches from Lemberg and Sadowski[14] allow predicting solvent effects on the reaction equilibrium and kinetics of esterification, but this model was limited to one catalyst concentration as catalyst effects on the kinetics were neglected. There are several approaches in the literature to integrate the proton concentration into kinetic models, most of them are empirical methods.[15–17] Other acknowledged kinetic models, for example, one parametrized by the temperature and the extent of conversion are available.[18] Overcoming such empirical models requires knowledge on catalyst interactions in the reactant mixture of an esterification. The thermodynamic model 'ePC-SAFT advanced'[19] allows modeling electrolytes in organic media by considering the change of dielectric properties of the medium at different conditions and the related change of solvation free energy of the ions. pH is an important influence factor on the reaction kinetics at various conditions since the catalyst properties (acid dissociation and proton activity) depend on the composition of a mixture. Thus, in the present work, ePC-SAFT advanced was used to predict catalyst dissociation and the respective proton activity along the reaction coordinate. This allowed predicting reaction kinetics as function of the catalyst concentration, of reactant concentration and of solvent addition.

Thermodynamic Fundamentals

Modeling Activity Coefficients with ePC-SAFT Advanced

ePC-SAFT advanced developed by Bülow et al.[14,19] is the most recent extension of the original equation of state PC-SAFT from Gross and Sadowski.[20] The electrolyte Perturbed-Chain Statistical Associating Fluid Theory (ePC-SAFT) established by Cameretti and Sadowski[21] and further developed by Held et al.[14,22] includes electrostatic long-range interactions among ions expressed by the Debye-Hückel theory to model electrolyte solutions. Based on this, an altered Born term to characterize solvation energies between charged components and the environment was added within the ePC-SAFT framework. The resulting model, ePC-SAFT advanced, calculates the dimensionless residual Helmholtz energy a^{res} of an electrolyte system as a sum of the following Helmholtz-energy contributions:

$$a^{res} = a^{hc} + a^{disp} + a^{assoc} + a^{DH} + a^{Born} \tag{2}$$

Classical PC-SAFT considers hard-chain repulsion of the reference system a^{hc} and perturbations to the hard chain caused by dispersive van der Waals forces and associative hydrogen-bonding forces, expressed by a^{disp} and a^{assoc}. In systems with charged species, two contributions were included additionally, namely the Debye-Hückel contribution a^{DH} to consider interionic electrostatic interactions and the modified Born term a^{Born} to describe electrostatic self-energy. Modelling electrolyte solutions requires accounting for the dipolar character of the medium. Therefore, an expression for the concentration-dependence of the relative dielectric constant is crucial for the electrostatic contribution to the solvation energy by means of the Born term. Detailed information about all contributions are described in the original PC-SAFT publication[20] and the most recent published works.[14,19] The activity coefficient for all reacting agents refer to the pure component state. It is defined as the ratio of the fugacity coefficient φ_i in the mixture and the fugacity coefficient of the pure component $\varphi_{0i}(x_i \rightarrow 1)$ and becomes equal to one at pure-component state, cf. Eq. (3). For ions, the rational activity coefficient $\gamma_i^{*,x}$ was used. In this work, we related to the infinite dilution in pure water and it is important to not change this reference state over the reaction coordinate. This property is calculated from the ratio of the fugacity coefficient φ_i of a component i at any desired condition (i.e., an ion infinitely diluted in organic solvent) and the fugacity coefficient of this component infinitely diluted in water $\varphi_i^{\infty,water}$ according to Eq. (3).

$$\gamma_i = \frac{\varphi_i(T,p,x)}{\varphi_{0i}(T,p,x_i=1)} \text{ and } \gamma_i^{*,x} = \frac{\varphi_i(T,p,x)}{\varphi_i^{\infty,water}(T,p,x_i=0)} \tag{3}$$

The fugacity coefficients φ_i depend on temperature, pressure, and composition, which is explicitly taken into account within ePC-SAFT advanced. In this work the thermodynamic activity of the proton is based on the mole fraction-based rational activity coefficient as follows

$$a_{H_3O^+}^{*,x} = x_{H_3O^+} \cdot \gamma_{H_3O^+}^{*,x} \tag{4}$$

Predicting activity coefficients requires ePC-SAFT parameters. All pure-component parameters and binary interaction parameters k_{ij} used in this work are listed in Table S1–S3. These were determined exclusively by fitting them to experimental phase-equilibrium data; reaction data was not used to fit any of the ePC-SAFT parameters.

Reaction Equilibria

Thermodynamic modeling of the esterification reaction kinetics in acid-catalyzed solutions requires simultaneously solving reaction kinetics of the esterification and of the dissociation equilibria of H_2SO_4. In addition to the esterification reaction (Eq.(1)), the following dissociation reactions take place in the liquid phase: first and second dissociation step of H_2SO_4 (5), (6), and dissociation of levulinic acid (7).

$$H_2SO_4 + H_2O \rightleftharpoons HSO_4^- + H_3O^+ \tag{5}$$

$$HSO_4^- + H_2O \rightleftharpoons SO_4^{2-} + H_3O^+ \tag{6}$$

$$LA + H_2O \rightleftharpoons LA^- + H_3O^+ \tag{7}$$

The esterification of LA is highly affected by the amount of dissociated H_2SO_4. Therefore, knowledge on the degree of dissociation of H_2SO_4 is crucial for the determination of H_3O^+

concentration. In this work, only the first dissociation step (5) was considered, while reactions (6) and (7) were neglected. Due to the significant amount of ethanol in the reaction mixture, it is not possible to measure reliably pH values. For that reason, an activity-based method was applied to model the dissociation equilibrium of H_2SO_4 in the reaction mixture. Reaction and dissociation equilibrium modeling requires the thermodynamic equilibrium constant K_{th}, which was calculated with the mole fractions of the reactants and products and their activity coefficients according to Eq. (8)

$$K_{th}(T,p) = \prod_i (x_i \cdot \gamma_i)^{\nu_i} = K_x(T,p,x) \cdot K_\gamma(T,p,x) \tag{8}$$

K_x denotes the mole-fraction ratio at equilibrium, or also known as apparent equilibrium constant. K_x changes under different conditions. The dependence of K_x on reaction conditions is taken into account by the activity coefficients γ_i. The resulting K_{th} depends only on temperature and pressure. Therefore, it takes the same value with or without additional solvent. Thus, once one value for K_{th} is known, ePC-SAFT predicted activity coefficients ($K_\gamma(T,p,x)$) allow determining the equilibrium position ($K_x(T,p,x)$). Following this concept, the dissociation of H_2SO_4 was predicted in this work at different reaction compositions. Therefore, pK_a values in water were used as obtained from the literature,[23] and the respective activity coefficients at the different compositions were predicted by ePC-SAFT advanced. The detailed methodology is described in the literature.[13] Further, also the K_{th} values of LA esterification for each temperature were determined using Eq. (8) by using equilibrium mole fractions of all listed experiments in Table S4 and the respective activity coefficients using ePC-SAFT advanced. The equilibrium constant K_{th} for each temperature is listed in Table S5. The standard reaction enthalpy $\Delta^R H^0$ was determined from the temperature-dependency of the K_{th} values. Addition of cosolvent decreases the equilibrium concentration caused by dilution. However, cosolvent also shifts the reaction equilibrium and the kinetics as such due to molecular interactions. In order to cancel out the dilution effect, the mole fraction of the ester product was normalized to the amount of additional cosolvent according to Eq. (9)

$$x_{ELA,norm} = \frac{x_{ELA}}{1 - x_{solvent}} \tag{9}$$

Kinetic Model I – State-of-the-Art Approach

Solvents might strongly influence reaction kinetics. This cannot be described by the classical concentration-based kinetic modeling approach, Eq. (10).

$$r = k \cdot c_A \cdot c_B \cdot - \frac{k}{K_a} \cdot c_C \cdot c_D \tag{10}$$

For that reason Lemberg and Sadowski[14] established a thermodynamic PC-SAFT framework to account for the molecular interactions between the reacting species and the solvent via activity coefficients. This enables the determination of solvent-independent kinetic constants k and the prediction of the solvent effects on reaction kinetics. Lemberg and Sadowski[14] studied the acid-catalyzed esterification reactions of acetic acid (HAc) and propionic acid (HProp) with ethanol in the solvents acetonitrile (ACN), tetrahydrofuran (THF) and N,N-dimethylformamide (DMF). Their model is based on the activity-based reaction kinetic equation, and it is expressed as follows:

$$r = k \cdot \gamma_A \cdot x_A \cdot \gamma_B \cdot x_B \cdot - \frac{k}{K_a} \cdot \gamma_C \cdot x_C \cdot \gamma_D \cdot x_D \tag{11}$$

for an equilibrium reaction of the type $A + B \rightleftharpoons C + D$. In this model, the reaction rate constant k is estimated with one experimental kinetic profile of a solvent-free reaction. Both, the activity coefficients and the mole fractions depend on the choice of solvent, whereas the calculated rate constant k keeps constant for each composition. This approach was also successfully used in kinetic studies of an esterification reaction with salt influence.[24] However, in contrast to the present work, the model of Lemberg and Sadowski was assuming constant catalyst concentration. The model performance at other catalyst concentrations is unknown.

Kinetic model II – Ion Effects on Reactants

Besides the interactions between the reacting agents, also the interactions between the acid (H_2SO_4) and its dissociated ions (HSO_4^-, H_3O^+) and the reacting agents and ions will influence the kinetics. ePC-SAFT advanced enables modeling these interactions in organic media by utilizing a modified Born term to consider electrostatic interactions of ionic compounds with their surrounding medium. In addition to that, Ascani et al.[25] successfully predicted pH values in multiphase multicomponent systems with ePC-SAFT advanced. Thus, we used this approach to calculate the activity coefficients of each ion in the reaction mixture and the ion influence on the activity coefficients of reacting agents. The resulting kinetic modeling approach is identical to Eq. (11), but the influence of the ions on the activity coefficients of the reacting agents was considered explicitly.

Kinetic model III – Approach Including the Proton Activity

Eq. (11) does not consider the influence of the catalyst concentration on kinetics. The idea of this work is to account for the catalyst by proton activity, for which proton-solvent interactions are required. ePC-SAFT advanced allows calculating proton activity, and the activity of H_3O^+-ions $a^{*,x}_{H_3O^+}$ was calculated for each of the reaction experiments. The resulting model to predict the catalyst concentration effect on the reaction kinetic is based on relating reaction rate by the proton activity $a^{*,x}_{H_3O^+}$ (Eq. (12)).

$$\frac{r}{a_{H_3O^+}^{*,x}} = k \cdot \gamma_A \cdot x_A \cdot \gamma_B \cdot x_B \cdot - \frac{k}{K_a} \cdot \gamma_C \cdot x_C \cdot \gamma_D \cdot x_D \quad (12)$$

In a first step, and similar to the state-of-the-art modeling, the rate constant k in equation (12) was fitted to one experiment to calculate all mole fractions and activity coefficients of the reacting agents, acid, and ions. Then, the corresponding $\frac{r}{a_{H_3O^+}^{*,x}}$ function was used for the prediction k at different conditions and solving simultaneously the dissociation equilibrium of H_2SO_4.

Results and Discussion

Esterification Equilibrium

As it is known from literature[14,26,27] an additional solvent usually decreases kinetics of esterification reactions and reduces the equilibrium concentration of a reaction product. In this work, the activities of reacting agents a_i at reaction equilibrium were predicted using ePC-SAFT advanced for different conditions. The activity-based thermodynamic equilibrium constants for all temperatures listed in Table S4 were calculated according to Eq. (8), and the result is shown in Figure 1.

The results in Figure 1 show a relatively high standard deviation. This is due to the fact that the reaction experiments scatter a lot, which is caused by several reasons. The mean value of K_{th} considering each single reaction equilibrium experiment is reported in Table S5, and the average values were used as input data into the kinetic calculations. Nevertheless, the temperature dependency of the equilibrium constant according to the Van't Hoff equation (Eq. S1) of all listed experiments in Table S4 is reasonable. The according reaction enthalpy at standard state $\Delta^R H^0 = 11.48\ kJ\ mol^{-1}$ is in good agreement with a reaction enthalpy value of Russo et al. (15.14 $kJ\ mol^{-1}$[28]). However, that the latter value is not a standard reaction enthalpy as it was obtained by using equilibrium concentrations instead of activities.

Reaction Kinetics

In a first step of this work, we applied kinetic model I from Lemberg and Sadowski[14] for the esterification of LA with EtOH. The prediction accuracy of the reaction equilibrium and kinetics of LA esterification in GVL cosolvent was validated. Further, we studied the limitations of the calculation approach and implemented a new modeling approach.

State-of-the-Art Kinetic Model I

In this section, the results of the reaction kinetics based on Eq. (11) are presented based on Lemberg and Sadowski's approach (model I). The results were obtained without accounting for the acid catalyst (H_2SO_4) and without the ions (H_3O^+, HSO_4^-). Lemberg and Sadowski[14] showed that the model could precisely predict solvent effects on the esterification of acetic acid with ethanol for all examined solvents.

In the following, it will be discussed whether the kinetic model I that is based on the activities of the neutral components allows predicting the solvent influence of GVL on the reaction kinetics of LA esterification. Figure 2 (left) shows the normalized ELA mole fraction over the reaction time for an experiment with and without GVL. In Figure 2 (right), two experiments with additional amount of GVL at different initial ratios of EtOH to LA are shown. It can be seen in Figure 2 that the predicted reaction rates match the experimental results reasonably. This confirms that kinetic model I combined with ePC-SAFT advanced allows predicting the GVL effect on the reaction rate and equilibrium of LA esterification using Eq. (11). The slight deviation between the prediction and experiments at

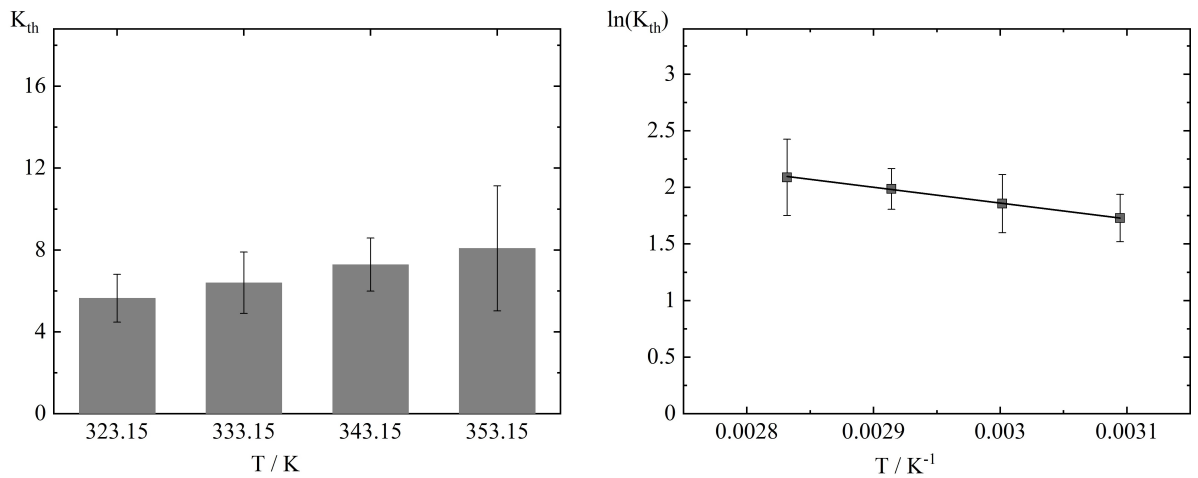

Figure 1. Left: Activity-based equilibrium constants K_{th} of LA esterification based on experimentally obtained K_x values from Baco et al.[13] with activity coefficients predicted by ePC-SAFT advanced using parameters summarized in Tables S1–S3. Right: Natural logarithmic function of K_{th} according to the Van't Hoff equation (Eq. S1), $y = -1397.75x + 6.05$.

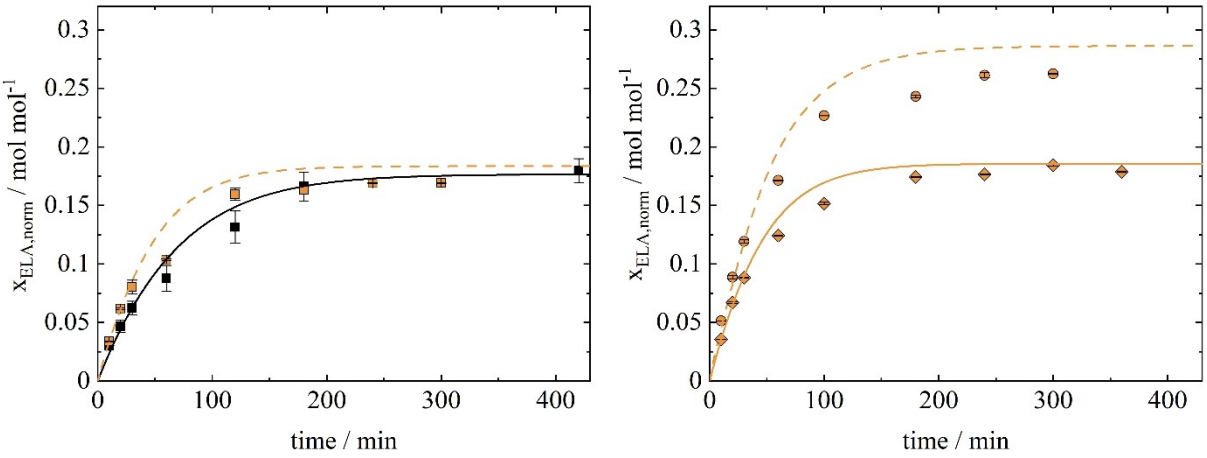

Figure 2. Normalized (see Eq.(9)) ethyl levulinate mole fraction of the esterification reaction in excess of EtOH (black) and with 14 mol% of GVL (orange). Experimental data:[13] EtOH1, black squares; GVL4, orange squares; GVL2, diamonds, EtOH:LA = 4; GVL5, circles, EtOH:LA = 2 (all conditions are listed in Table S4). Error bars give the standard deviations out of three measurements. Lines are modeling using ePC-SAFT advanced according to Eq. (11) using the parameters from Tables S1–S3. Solid lines: *k* was fitted to experimental values using Eq. (11), dashed lines: predictions using model I.

equilibrium results from the uncertainty of the equilibrium constant, cf. Figure 1. Besides the solvent influence, the effect of initial concentration ratios of EtOH to LA was also predicted very well, even at the presence of GVL cosolvent (Figure 2 – right). One experimental kinetic curve was required to determine the rate constant *k*, and *k* was then considered to be solvent-independent in the predictions. The predictions were performed for different conditions, such as initial ratios of EtOH:LA and adding GVL cosolvent. However, kinetic model I is only valid at constant catalyst concentration, as catalyst influence on the reacting agents is not included in the kinetic model I. This is briefly illustrated in the SI, cf. Section S3 and Figure S1. The conventional solution to this shortcoming is to fit new rate constants *k* for each experiment with a different catalyst concentration, which is not in the focus of this work.

Kinetic Model II – Influence of Ions on Reactants

The big drawback of the kinetic model I described in Section 3.2.1 is the inability to describe the effect of catalyst concentration on reaction kinetics. The idea behind model II was to account for the influence of ions originating from the catalyst on the reactant activities. Prior to this, knowledge on the dissociation equilibrium of the acid catalyst was needed. Therefore, an activity-based equilibrium constant using literature pK_a value of H_2SO_4 in water[23] ($pK_a = -3$) the first dissociation step of H_2SO_4 was calculated. The second dissociation step of H_2SO_4 was neglected. The concentrations of H_3O^+ and HSO_4^- in the reaction mixtures are listed in Table S5. To summarize the results, we found that these ions only contribute to <1 mol% of the overall acid concentration at the initial reaction conditions. This result is in agreement what we found in previous work on ePC-SAFT predicted pK_a values in different solvents compared to experimental data.[13] The ability to predict the solvent-dependent acid dissociation over the reaction coordinate then allowed us modeling the activity coefficients of the reacting agents including interactions to the catalyst species. The activity coefficients calculated with and without influence of the catalyst species are presented in Figure 3.

Figure 3 shows that the acid species (neutral H_2SO_4 and ions H_3O^+ and HSO_4^-) do not strongly influence the activity coefficients of the reacting agents. As a result the equilibrium as well as the kinetics using Eq. (11) do not change much upon addition of the rather low catalyst concentration, and the predicted *k* values of modeling approach I and II are very similar. This is an expected result as by the very low

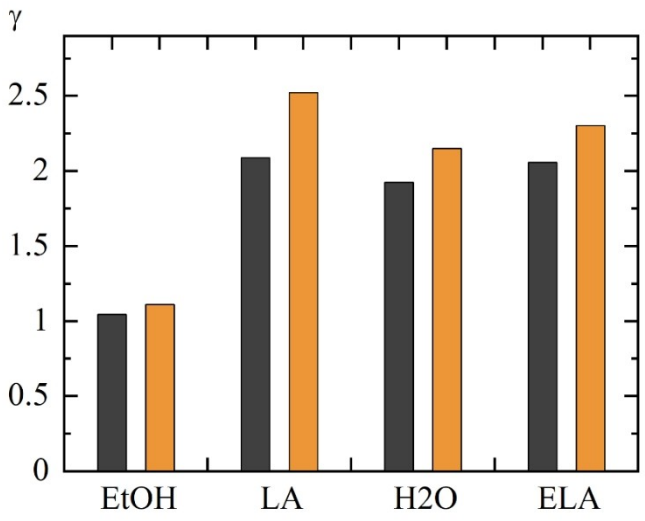

Figure 3. Activity coefficients of the reacting agents belonging to the equilibrium mole fractions of the experiment GVL4 listed in Table S4. Grey: excluding the presence of acid and ions (kinetic modeling approach I), orange: including effect of acid and ions on the activity coefficients (kinetic modeling approach II) using the ePC-SAFT parameters from Tables S1–S3.

concentration of catalyst used in the experiments (Table S4, EtOH1). To conclude, a precise kinetic model of the acid-catalyzed esterification reaction must not only account for the acid effect on the interactions of reacting agents, rather it must consider the effect of catalyst on reaction rate. Therefore, proton activity along the reaction coordinate is required.

Kinetic Model III – Influence Proton Activity on Reaction Rate

In this section, a new calculation approach considering the catalyst concentration and dissociation equilibrium of the catalyst in the kinetic expression is presented. Kinetic model III accounts for dissociation of H_2SO_4 in the reaction mixture combined with the calculation of the proton activity using ePC-SAFT advanced. In the literature, catalyst or proton concentration has already been included within kinetic expressions.[15,16,29,30] However, in this work we applied an activity-based approach instead of a concentration-based approach to account for catalyst effects on reaction rate. In a first step, proton activity was predicted with ePC-SAFT advanced over the reaction coordinate as shown in Figure 4.

Figure 4 shows the proton activity of different experiments at three different catalyst concentrations. The proton activity was calculated with ePC-SAFT advanced using the mole fraction of H_3O^+ ions (obtained from solving the dissociation equilibria) and the rational activity coefficient $\gamma^{*,x}_{H_3O^+}$. It can be observed that proton activity is higher for higher initial catalyst concentrations, which is an expected result. However, proton activity does not double upon doubling the concentration of catalyst. Further, adding GVL solvent does not have a significant effect on the proton activity compared to GVL-free reactions. Available values for proton activity then allowed establishing the quotient of reaction rate over proton activity (Eq.(12)). The resulting curves of $\frac{r}{a^{*,x}_{H_3O^+}}$ are shown in Figure 5, and the relation turns out to be a promising tool for a predictive kinetic model as all the curves fall back to one line for one isotherm.

Figure 5 shows the ratio of reaction rate r to proton activity $a^{*,x}_{H_3O^+}$ over the reaction coordinate of LA esterification. The graph contains each experiment listed in Table S4. Promisingly, all the curves are equal within uncertainty at isothermal conditions despite the fact that each experiment contained different catalyst concentration, different initial molar ratios, and w/o GVL cosolvent. This is considered to be suitable for establishing a predictive model. Therefore, Eq. (12) is rearranged to the rate constant k (Eq. (13)).

$$k = \frac{r}{a^{*,x}_{H_3O^+}} \cdot \left(\gamma_A \cdot x_A \cdot \gamma_B \cdot x_B \cdot - \frac{1}{K_a} \cdot \gamma_C \cdot x_C \cdot \gamma_D \cdot x_D\right)^{-1} \quad (13)$$

Eq. (13) was used to determine the rate constants for each experiment. Compared to the procedure mentioned before (cf. Figure 4) the rate constant was fitted only to one $\frac{r}{a^{*,x}_{H_3O^+}}$ curve at each temperature. That is, only one experimental kinetic curve was necessary to determine k, which was then used to predict kinetic curves at different conditions regarding catalyst concentration of reacting agent concentration or presence of GVL cosolvent. The modeling results for some selected rate constants k are shown in Figure 6 (all results are listed in Table S6).

Figure 6 compares the rate constants k between kinetic model I and kinetic model III, and the experiments behind contained different amount of catalyst. Kinetic model I is only

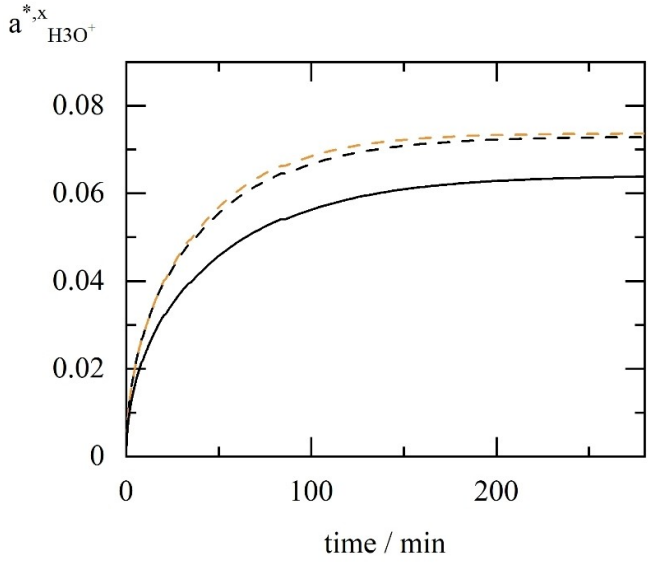

Figure 4. *Proton activity ($a^{*,x}_{H_3O^+}$) vs. reaction time of LA esterification of three experiments at 323 K and 1 bar. Black: GVL-free with excess of EtOH; orange: 14* mol% *GVL; dashed lines: $x_{H_2SO_4} = 0.006$ (GVL4, EtOH1), solid line: $x_{H_2SO_4} = 0.003$ (EtOH6). All lines are ePC-SAFT advanced calculations using the parameters from Tables S1–S3.*

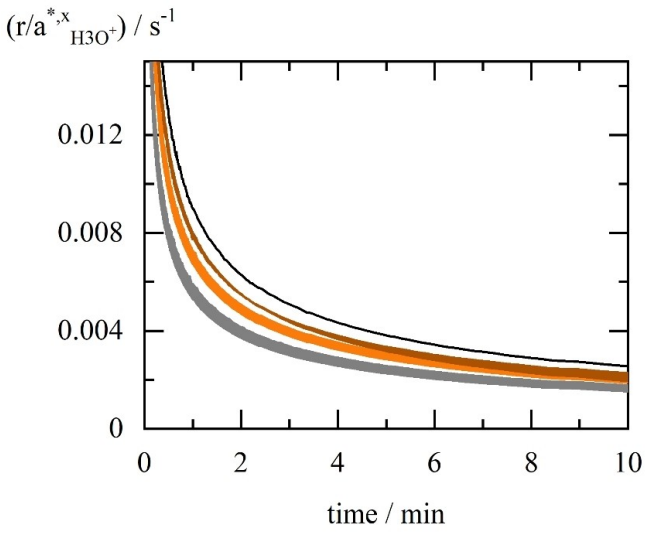

Figure 5. Ratio of reaction rate r to proton activity $a^{*,x}_{H_3O^+}$ over the reaction time for all experimental conditions from Table S4 clustered at different temperatures (grey: 323.15 K, orange: 333.15 K, red: 343.15 K, black 353.15 K). The uncertainty is represented by the thickness of the lines. All lines are ePC-SAFT advanced predictions using the parameters from Tables S1–S3.

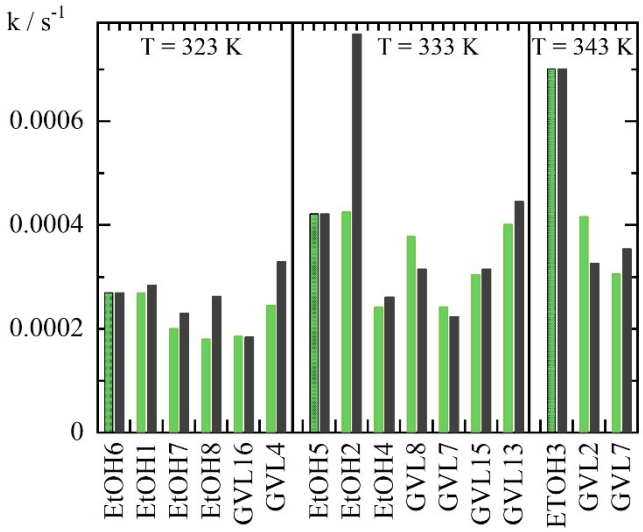

Figure 6. Rate constants *k* for selected experimental conditions listed in Table S6. Green: predicted rate constants using kinetic model III according to Eq. (13). The $\frac{a^{*}_{x}}{a^{*}_{H_3O^+}}$ curves of the shaded bars (EtOH6, EtOH5, EtOH3) were used as reference into ePC-SAFT advanced with the parameters from Tables S1–S3. Grey: each rate constant was fitted to a single kinetic curve using kinetic model I and the experimental data from Table S4.

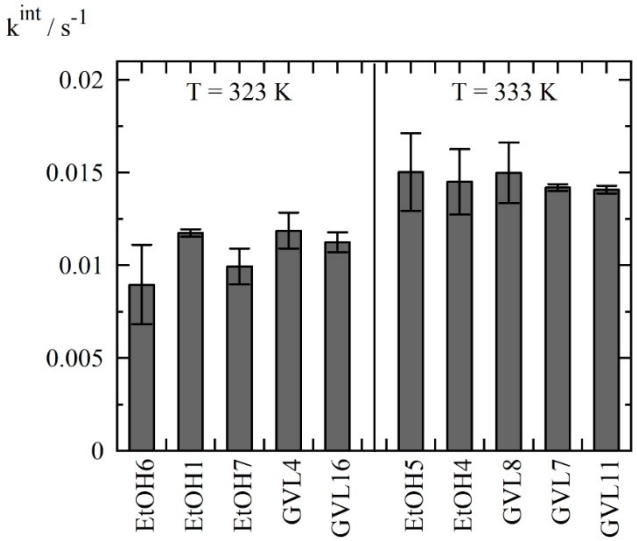

Figure 7. Intrinsic rate constants for selected experimental conditions (cf. Table S4) calculated using ePC-SAFT advanced according to Eq. (14). Error bars result from the experimental uncertainties shown in Figure S3.

valid at one catalyst concentration. Thus, the *k* values of kinetic model I was fitted to each kinetic curve with a new catalyst concentration. Obviously, the *k* values obtained by this are in good agreement to the *k* values of the kinetic model III, which is predictive in catalyst concentration. This proves the feasibility of kinetic model III towards predicting the influence of catalyst concentration on reaction rates. In a further step, the *k* values shown in Figure 6 were related to proton activity in order to obtain "intrinsic" rate constants k^{int} by multiplying with proton activity according to Eq. (14).

$$k^{int} = k \cdot a^{*,x}_{H_3O^+} = r \cdot (\gamma_A \cdot x_A \cdot \gamma_B \cdot x_B \cdot - \frac{1}{K_a} \cdot \gamma_C \cdot x_C \cdot \gamma_D \cdot x_D)^{-1} \quad (14)$$

The resulting k^{int} represents a reaction rate constant that is independent of solvent, of concentrations, and of catalyst. The resulting k^{int} values are shown in Figure 7.

Interestingly, all the intrinsic rate constants k^{int} related with proton activity according to Eq. (14) are equal within uncertainty for isothermal conditions. This is the reason for the result shown in Figure 6 that allows predicting the kinetics of the LA esterification at any conditions. In order to describe the temperature dependency of the intrinsic rate constants, the Arrhenius approach was used with k^{int} as input data, cf. Figure S4, yielding an activation energy $E_A = 30.28\ kJ\ mol^{-1}$, which fits to the literature data from Russo et al.[28] The deviation within the rate constants origins from experimental uncertainties, cf. Figure S3, which then are found in the modeling results.

Quantitative evaluation of the *k* values was obtained by the average absolute relative deviation (AARD) related to the mean value of experimental data. AARD1 relates to the ePC-SAFT advanced predictions used by kinetic model III, Eq. (12), while AARD2 corresponds to the classically-obtained *k* values by fitting to kinetic curves at different catalyst concentrations (kinetic model I, Eq. (11)):

$$AARD1 = 100 \cdot \frac{1}{NP} \cdot \sum_{n=1}^{NP} \left| 1 - \frac{x_n^{ePC-SAFT,\ fitted}}{x_n^{exp}} \right| \quad (15)$$

$$AARD2 = 100 \cdot \frac{1}{NP} \cdot \sum_{n=1}^{NP} \left| 1 - \frac{x_n^{ePC-SAFT,\ predicted}}{x_n^{exp}} \right| \quad (16)$$

Here, $x_n^{ePC-SAFT}$ represents the mole fraction of ELA obtained by kinetic model I with fitted *k* values (Eq. (15)) and predicted kinetic model III *k* values (Eq. (16)) using ePC-SAFT advanced, and x_n^{exp} denotes the respective experimental value. NP denotes the sum of the available experimental data points *n*. The calculated AARD1 and AARD2 values based on the resulting mole fraction of ELA for each experiment are listed in Table 1.

It is evident to see from the AARD values that fitting a new kinetic constant to each of the experimental kinetic curve of LA esterification (kinetic model I) is more accurate than predicting the kinetic curves using kinetic model III, which uses only one kinetic curve for model validation and then predicts all other kinetic curves. This is an expected result. Still, the general deviation of both models to the experimental results is in the order of magnitude of 10%. Some results show (e.g., Figure S3) underpredicted kinetics at reaction times of 60–200 min, which results in quite high AARD values. Nevertheless, the kinetic curves are usually in good agreement with the experimental data at the very beginning of the reactions. Thus, kinetic model III proves to be feasible for the prediction of reaction rates at all reaction conditions considered in this work. Kinetic model III

Table 1. Calculated AARD for the resulting mole fraction of ethyl levulinate. AARD1 corresponds to kinetic model I, Eq. (11) and (15), while AARD2 corresponds to kinetic model III, Eq. (12) and (16).

Exp.	AARD1 /[%]	AARD2 /[%]
ETOH6	10.78	–
ETOH1	6.54	6.40
ETOH7	14.52	13.96
ETOH8	5.14	11.46
GVL4	9.82	12.32
GVL16	15.39	15.04
ETOH5	7.68	–
ETOH2	9.52	35.15
ETOH4	10.21	13.57
GVL8	12.26	15.01
GVL3	17.53	18.52
GVL7	7.25	12.57
GVL13	4.73	6.06
GVL15	7.71	9.43
ETOH3	10.70	–
GVL2	6.37	8.71
GVL5	11.35	14.64
Avg.	9.85	13.77

combines the benefits of the model developed from Lemberg and Sadowski[14] to account for the reacting agent activities and the most recent ePC-SAFT advanced development by Bülow et al.[19] to account for the proton activity.

General Importance of Activity-Based Approaches

This section outlines the importance and the benefits of an activity-based kinetic approach such as the newly developed kinetic model III. In the following, the different kinetic approaches from the literature (classical concentration based, activity-based according to Lemberg and Sadowski[14]) are compared to the newly developed kinetic model III. Therefore, a selection of kinetic constants for experiments with GVL solvent and with varying catalyst concentrations are shown in Figure 8.

Figure 8 illustrates the influences of GVL cosolvent and of catalyst concentration on the rate constants k for four selected experiments (EtOH1 and GVL4 at 323 K and GVL7 and GVL11 at 333 K). As required for the kinetic model III, k^{int} must be independent of solvent and catalyst; obviously, this has been successfully reached within our work. Further, the concentration-based approach is expected to require k values that depend on all different conditions, such as concentration, cosolvent addition and catalyst variation. Obviously, this expected result could be proven according to the results in Figure 8. Another expected result is the ability of Lemberg and Sadowski's kinetic model I to predict (co)solvent effects on k. As it can be observed, we indeed obtained constant k values for EtOH1 and GVL4, where the only difference is the additional presence of 14 mol% of GVL cosolvent in the experiment GVL4 while keeping catalyst concentration constant. Finally, the two experiments GVL7 and GVL11 are considered, which were conducted at different catalyst concentrations. As expected, the kinetic model I fails in predicting the catalyst effect on kinetics as the k values do significantly depend on catalyst. Only the newly developed kinetic model III allows using kinetic constants that do not depend on the composition at all at constant temperature, and these values were denoted k^{int}.

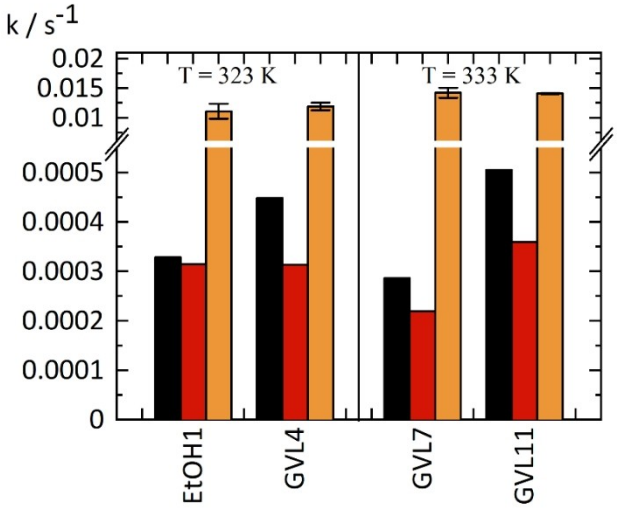

Figure 8. Rate constants for LA esterification at two different temperatures obtained by different kinetic models. Black: k obtained by a concentration-based approach (Eq. (10)), red: k obtained by the activity-based approach according to model I (Eq.(11)), orange: k^{int} obtained by newly developed kinetic model III (Eq.(12)).

Conclusions

In this work, we compared different kinetic models to describe the influences of GVL cosolvent and catalyst on the kinetics of LA esterification with ethanol at different temperatures. We successfully applied the thermodynamic activity-based approach Lemberg and Sadowski[14] for the prediction of solvent effects on both, reaction equilibrium and reaction rates of the esterification reaction. It turned out that yield and reaction rate was increased by using 14 mol% GVL as an additional solvent. Further, we utilized the recently developed equation of state ePC-SAFT advanced to calculate the dissociation of H_2SO_4 in the reaction mixture. This enabled predicting proton activity coefficients in order to relate reaction rate to proton activity. Combining this with the existing model from Lemberg and Sadowski was successfully applied to predict kinetics as function of catalyst concentration, and the predictions were validated by experimental literature data. The approach was used to provide "intrinsic" kinetic constants, which are independent of solvent, concentrations, and catalyst. The main advantage of the presented kinetic approach is to reduce significantly the number of parameters in kinetic expressions to describe the reaction kinetics in the multivariant space of solvent, concentration ratios, and catalyst concentration. Only one experimental kinetic curve was required for the prediction of the kinetics at any different condition at constant temperature. In contrast, state-of-the-art methods require one reaction constant per catalyst concentration. To conclude, thermody-

namic modeling of both, dissociation equilibrium of the acid catalyst and activity-based treatment of the LA esterification using ePC-SAFT advanced enabled the successful prediction of the equilibrium compositions and kinetics as function of temperature, concentration, cosolvent addition and catalyst concentration.

Acknowledgements

This research was funded, in whole or in part, by the DFG (German Research Foundation) and the ANR (French National Research Agency) within the project MUST (MicroflUidics for Structure-reactivity relationships aided by Thermodynamics & kinetics) [ANR-20-CE92-0002-01 – Project number 446436621] and HE 7165/10-1. Open Access funding enabled and organized by Projekt DEAL.

Conflict of Interest

The authors declare no conflict of interest.

Data Availability Statement

The data that support the findings of this study are available in the supplementary material of this article.

Keywords: catalyst effect · ePC-SAFT advanced · GVL · proton activity · solvent effect · thermodynamics

[1] J. J. Bozell, *ACS Symp. Ser.* **2001**, *784*.
[2] F. D. Pileidis, M.-M. Titirici, *ChemSusChem* **2016**, *9*, 562–582.
[3] S. Nanda, R. Azargohar, A. K. Dalai, J. A. Kozinski, *Renewable Sustainable Energy Rev.* **2015**, *50*, 925–941.
[4] D. M. Alonso, J. Q. Bond, J. A. Dumesic, *Green Chem.* **2010**, *12*, 1493.
[5] J. C. Serrano-Ruiz, J. A. Dumesic, *Energy Environ. Sci.* **2011**, *4*, 83–99.
[6] J.-P. Lange, W. D. van de Graaf, R. J. Haan, *ChemSusChem* **2009**, *2*, 437–441.
[7] E. Ahmad, M. I. Alam, K. K. Pant, M. A. Haider, *Green Chem.* **2016**, *18*, 4804–4823.
[8] D. R. Fernandes, A. S. Rocha, E. F. Mai, C. J. Mota, V. Da Teixeira Silva, *Appl. Catal. A* **2012**, *425–426*, 199–204.
[9] K. Y. Nandiwale, S. K. Sonar, P. S. Niphadkar, P. N. Joshi, S. S. Deshpande, V. S. Patil, V. V. Bokade, *Appl. Catal. A* **2013**, *460–461*, 90–98.
[10] H. J. Bart, J. Reidetschlager, K. Schatka, A. Lehmann, *Ind. Eng. Chem. Res.* **1994**, *33*, 21–25.
[11] M. A. Mellmer, C. Sener, J. M. R. Gallo, J. S. Luterbacher, D. M. Alonso, J. A. Dumesic, *Angew. Chem. Int. Ed.* **2014**, *53*, 11872–11875; *Angew. Chem.* **2014**, *126*, 12066–12069.
[12] Y. Gu, F. Jérôme, *Chem. Soc. Rev.* **2013**, *42*, 9550–9570.
[13] S. Baco, M. Klinksiek, R. Ismail Bedawi Zakaria, E. Antonia Garcia-Hernandez, M. Mignot, J. Legros, C. Held, V. Casson Moreno, S. Leveneur, *Chem. Eng. Sci.* **2022**, *260*, 117928.
[14] M. Lemberg, G. Sadowski, *ChemPhysChem* **2017**, *18*, 1977–1980.
[15] R. Tesser, M. Di Serio, M. Guida, M. Nastasi, E. Santacesaria, *Ind. Eng. Chem. Res.* **2005**, *44*, 7978–7982.
[16] A. V. Chernysheva, V. M. Chernyshev, P. V. Korolenko, V. A. Taranushich, *Russ. J. Appl. Chem.* **2008**, *81*, 1813–1817.
[17] G. Jyoti, A. Keshav, J. Anandkumar, S. Bhoi, *Int. J. Chem. Kinet.* **2018**, *50*, 370–380.
[18] S. Hanafi, D. Trache, R. Meziani, H. Boukeciat, A. F. Tarchoun, A. Abdelaziz, A. Mezroua, *FirePhysChem* **2022**.
[19] M. Bülow, M. Ascani, C. Held, *Fluid Phase Equilib.* **2021**, *535*, 112967.
[20] J. Gross, G. Sadowski, *Ind. Eng. Chem. Res.* **2001**, *40*, 1244–1260.
[21] L. F. Cameretti, G. Sadowski, J. M. Mollerup, *Ind. Eng. Chem. Res.* **2005**, *44*, 3355–3362.
[22] C. Held, T. Reschke, S. Mohammad, A. Luza, G. Sadowski, *Chem. Eng. Res. Des.* **2014**, *92*, 2884–2897.
[23] *pKa data compiled by R. Williams*, **2019**.
[24] D. Pabsch, J. Lindfeld, J. Schwalm, A. Strangmann, P. Figiel, G. Sadowski, C. Held, *Chem. Eng. Sci.* **2022**, *263*, 118046.
[25] M. Ascani, D. Pabsch, M. Klinksiek, N. Gajardo-Parra, G. Sadowski, C. Held, *Chem. Commun. (Camb.)* **2022**.
[26] F. Huxoll, F. Jameel, J. Bianga, T. Seidensticker, M. Stein, G. Sadowski, D. Vogt, *ACS Catal.* **2021**, *11*, 590–594.
[27] F. Huxoll, A. Kampwerth, T. Seidensticker, D. Vogt, G. Sadowski, *Ind. Eng. Chem. Res.* **2022**, *61*, 2323–2332.
[28] V. Russo, V. Hrobar, P. Mäki-Arvela, K. Eränen, F. Sandelin, M. Di Serio, T. Salmi, *Top. Catal.* **2018**, *61*, 1856–1865.
[29] P. Delgado, M. T. Sanz, S. Beltrán, *Chem. Eng. J.* **2007**, *126*, 111–118.
[30] D.-J. Tao, Y.-T. Wu, Z. Zhou, J. Geng, X.-B. Hu, Z.-B. Zhang, *Ind. Eng. Chem. Res.* **2011**, *50*, 1989–1996.

Manuscript received: October 1, 2022
Revised manuscript received: October 20, 2022
Accepted manuscript online: October 20, 2022
Version of record online: November 16, 2022